Redox Biology 53 (2022) 102349

Contents lists available at ScienceDirect

Redox Biology

journal homepage: www.elsevier.com/locate/redox

Ethyl carbamate triggers ferroptosis in liver through inhibiting GSH synthesis and suppressing Nrf2 activation

Yang Xu [a,1], Yuting Li [a,1], Jiaxin Li [a], Wei Chen [a,b,*]

[a] Department of Food Science and Nutrition, College of Biosystems Engineering and Food Science, Zhejiang University, Hangzhou, 310058, China
[b] Ningbo Research Institute, Zhejiang University, Ningbo, 315100, China

ARTICLE INFO

Keywords:
Ethyl carbamate
Ferroptosis
Lipid peroxidation
GSH depletion
Nrf2

ABSTRACT

Humans are inevitably exposed to ethyl carbamate (EC) *via* consumption of fermented food and beverages. EC, known as an environmental toxin, can cause oxidative stress-mediated severe toxicity, but the underlying mechanisms remain unveiled. Ferroptosis is a newly identified ROS-mediated non-apoptotic cell death characterized by iron accumulation and excessive lipid oxidation. In this study, we first found that EC triggered ferroptosis in liver cells by detection of decreased cell viability, GSH, GPX4 and Ferritin levels, as well as increased iron and MDA contents. Ferroptosis inhibitor ferrostatin-1 (Fer-1) pretreatment rescued ferroptotic damage, indicating that ferroptosis was critical for EC-caused cell death. Furthermore, GSH synthesis precursor *N*-acetylcysteine displayed significant anti-ferroptotic properties and we suggested that GSH depletion might be the main cause of ferroptosis under EC exposure. EC-triggered GSH depletion mainly depended on suppressed GSH synthesis *via* inhibition of SLC7A11 and GCLC expressions. Notably, EC blocked Nrf2 activation by repression of phosphorylation modification and nuclear translocation, which further resulted in ferroptosis occurrence. We also observed EC-induced liver dysfunction and inflammation, accompanied with oxidative stress, ferroptosis and downregulated Nrf2 signaling in Balb/c mice, which could be effectively reversed by Fer-1 and tBHQ pretreatment. Together, our study indicated that ferroptosis is a new mechanism for EC-caused toxicity, which was attributed to Nrf2 inactivation and GSH depletion.

1. Introduction

Ethyl carbamate (EC), also called urethane, is naturally produced and presented in high levels during the fermentation of food and beverages [1,2]. Exposure of humans to EC often occurs inevitably *via* routine dietary or consumption of cigarettes. EC was used as a hypnotic and antitumor drug in humans and laboratory animals during the nineteenth century before it was found to cause lung adenomas in mice for the first time in 1943 [3]. Subsequent research has demonstrated that EC may generate multiple-site tumor, including tumors in lung, liver, skin and other organs [4,5]. Therefore, it has been categorized as probably carcinogenic to humans (Group 2A) by the World Health Organization's International Agency for Research on Cancer (IARC) in 2010. Besides, EC exposure results in oxidative stress in various cell lines, such as RAW 264.7 macrophages, A549 lung epithelial cells, L02 liver cells and Caco-2 colon cells [6–9]. Although reactive oxygen species (ROS) overproduction has been further proved to be the main reason for EC-triggered toxicity, the detailed mechanism of the cytotoxicity under EC exposure has not been completely clarified.

ROS, containing an array of chemical species produced by incomplete reduction of oxygen, serve as singling molecules and is critical for development and proliferation of living organisms [10]. Oxidative stress can be denoted as elevated ROS generation, further leading to molecular damage and organelle dysfunction [11]. Elevation of lipid-based ROS, particular lipid hydroperoxides, may trigger ferroptosis process. Ferroptosis is a recently discovered form of cell death characterized by lipid peroxidation and iron overload, which also exhibits completely different features of morphology, biochemistry and genetic regulation compared with other forms of reprogrammed cell death [12]. Ferroptosis acts as a dual role in health and disease [13]. Ferroptosis under normal physiological conditions can decrease damaged cells and maintain homeostasis. However, ferroptosis also promotes occurrence and development of

* Corresponding author. Department of Food Science and Nutrition, College of Biosystems Engineering and Food Science, Zhejiang University, No.866 Yuhangtang Road, Xihu District, Hangzhou, 310058, China.
E-mail address: zjuchenwei@zju.edu.cn (W. Chen).
[1] These authors contributed equally to this work.

https://doi.org/10.1016/j.redox.2022.102349
Received 28 April 2022; Accepted 19 May 2022
Available online 22 May 2022

cancer, neurodegenerative disorders, inflammation and diabetes [14–17]. Recently, increasing studies also demonstrate that ferroptosis might be involved in toxicity induced by environmental irritants and harmful chemicals [18–20].

Lipid peroxidation of ferroptosis is mainly driven by decreased glutathione peroxidase 4 (GPX4) levels. GPX4, a glutathione (GSH) and selenium-dependent glutathione peroxidase, functions as the major phospholipid hydroperoxidase to suppress lipid ROS production [21]. GSH is a critical intracellular antioxidant and plays a central role in GPX4 activity as the vital substrate in reduction reaction of hydroperoxides [22]. The biosynthesis of GSH is sustained by amino acid antiporter SLC7A11-modulated cystine transport and GCL-mediated conjunction of cysteine and glutamate. Hence, cystine-GSH-GPX4 axis is regarded as the mainstay in ferroptosis regulation [23]. EC-triggered toxicity in liver cell is related to excess ROS generation and GSH depletion [9]. Therefore, we inferred that ferroptosis might occur in EC-treated L02 cells, which may be ascribe to inhibition of GSH synthesis and GPX4 expression.

Nuclear factor erythroid 2 related factor 2 (Nrf2, also named as NFE2L2) is critical for oxidative stress defense and activated *via* translocation from cytoplasm to nucleus. Nrf2 maintains redox balance by modulating related genes, such as *GSS*, *GPX4*, *GCLC* and *SLC7A11*, and also acts as a master transcription factor that can regulate target genes in iron homeostasis [24]. Studies have elucidated that inhibition of Nrf2 signaling can promote ferroptosis process, indicating that Nrf2 exhibits anti-ferroptotic functions [14,25]. Hence, we proposed that EC might trigger ferroptotic cell death *via* inhibtion of Nrf2 signaling.

In the present study, we analyzed effects and underlying mechanisms of EC-induced toxicity in human liver cells L02 and liver tissues. Our study suggested that EC exposure caused Nrf2 inactivation and GSH depletion, further leading to initiation of ferroptosis and liver dysfunction.

2. Materials and methods

2.1. Regents

Ethyl Carbamate (EC), paraformaldehyde, glutaraldehyde, N-acetylcysteine (NAC), Ferrostain-1 (Fer-1), 3-(4,5-dimthyl-2-thiazolyl)-2,5-diphenyl-2-H-tetra-zolium bromide (MTT), tert-Butylhydroquinone (tBHQ), trypan blue, DMSO and Tris were obtained from the Sigma-Aldrich (St. Louis, MO, USA). All other reagents used were of analytical grade.

2.2. Cell culture

The human hepatic cell line L02 were purchased from the Cell Bank of Type Culture Collection of Chinese Academy of Sciences. Cells were cultured in RPMI 1640 medium with 10% FBS (fetal bovine serum) and antibiotics (100 units/mL penicillin and streptomycin) at 37 °C in the presence of 5% CO_2.

2.3. Cell viability assays

Cell viability was detected by MTT assay with 4 replicates according to previous study [26]. Changes in cell viability were determined using a series of EC concentrations on 24 h exposure. In the rescue experiments, Fer-1 (5 μM), NAC (2 mM) or tBHQ (10 μM) were added in cells 1 h before EC treatment for 24 h. The reaction product formazan was dissolved in DMSO and detected at 490 nm.

2.4. Animal treatment

Specific pathogen free (SPF) male BALB/c mice (6–8 weeks) were purchased from the Zhejiang Chinese Medical University. After 7-day adaption, mice were divided randomly into 4 groups: control, low-dose of EC (50 mg/kg bw), medium-dose of EC (150 mg/kg bw) and high-dose of EC (450 mg/kg bw), with 10 animals in each group. EC was administrated by oral gavage. All mice were kept in a controlled environmental condition and allowed *ad libitum* to food and water. After 28-day consecutive administration with EC, the mice were sacrifice following 12 h fasting.

In the rescue experiments, male BALB/c mice were divided randomly into 6 groups: control, EC (450 mg/kg bw), Fer-1 (1 mg/kg bw) + EC, tBHQ (20 mg/kg bw) + EC, Fer-1 (1 mg/kg bw), tBHQ (20 mg/kg bw), with 10 animals in each group. Mice were received intraperitoneal (i.p.) injections of Fer-1 (1 mg/kg bw, dissolved in 1% DMSO+50% PEG 300+5% Tween 80) or tBHQ (20 mg/kg bw, dissolved in 1% DMSO solution), followed by oral administration of EC (450 mg/kg bw, dissolved in distilled water) after 30 min. In control, Fer-1 and tBHQ groups, mice were i.p. received 1% DMSO+50% PEG 300+5% Tween 80 solution, Fer-1 (1 mg/kg bw) solution and tBHQ (20 mg/kg bw) solution, respectively, followed by oral administration of distilled water. After 21-day consecutive administration, the mice were sacrifice following 12 h fasting.

Blood was collected and centrifuged for serum collection. Liver tissues were collected and weighed. Serum and liver samples were stored at −80 °C for further investigation. All protocols were performed following the guidance of the Institutional Animal Care and Use Committee of Zhejiang Chinese Medical University with the Approval of Animal Ethical and Welfare No. IACUC-20201228-07 (EC toxicity experiments) and IACUC-20211025-13 (rescue experiments).

2.5. Measurement of reduced GSH, MDA and SOD

Lysates of cells and liver tissues were obtained using RIPA Lysis Buffer (Beyotime, China) and reduced glutathione levels measured with Reduced GSH Detection Kit (Nanjing Jincheng, China). MDA and SOD were detected using Lipid Peroxidation MDA Assay Kit (Beyotime, China) and Total Superoxide Dismutase Assay Kit (Beyotime, China) respectively according to the manufacturer's instructions.

2.6. Iron content determination

Lysates of cells and liver tissues were first obtained using RIPA Lysis Buffer (Beyotime, China). Contents of iron in serum and liver lysates were detected following manufacturer's instructions of Serum Iron Assay Kit (Nanjing Jincheng, China) and Tissue Iron Assay Kit (Nanjing Jincheng, China), respectively. Iron concentrations in cell lysates were tested using Intracellular Iron Colorimetric Assay Kit (Applygen, China).

2.7. Transmission Electron Microscopy (TEM) assays

TEM assay was conducted according to previous study [27]. Liver samples were first fixed with 2.5% glutaraldehyde for 24 h at 4 °C. Then, the samples were washed three times with PBS and fixed with 1% osmium tetroxide for 2 h. After that, liver samples were dehydrated in a graded series of ethanol and acetone, followed by embeding in Spurr resin. Ultrathin sections were obtained and stained with uranyl acetate and lead citrate. Images were analyzed using Hitachi model H-7650 TEM.

2.8. Western blot

Liver tissues and L02 cells were homogenized in ice-cold RIPA Lysis Buffer (Beyotime, China) with PMSF. Concentrations of protein samples were detected by BCA protein assay (Beyotime, China). Western blotting was performed as previously described [27]. Protein samples with equal amounts were separated using SDS/PAGE gels and then transferred to polyvinylidene difluoride (PVDF) membrane. After being blocked with 5% BSA for 1 h, membranes were incubated with specific primary antibodies overnight at 4 °C. The primary antibodies were shown as

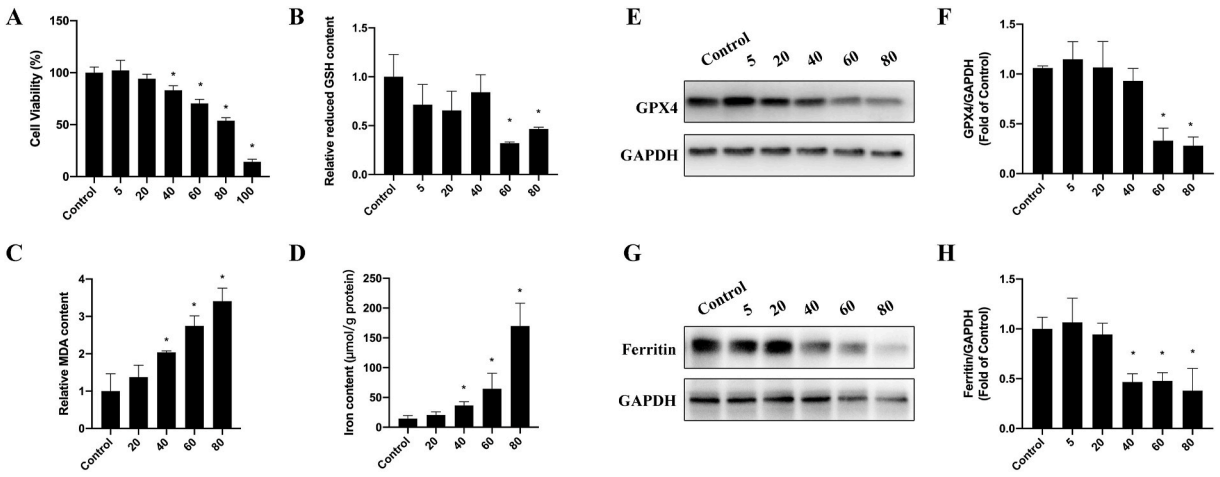

Fig. 1. Ethyl carbamate triggered ferroptosis in L02 cells. Cells were incubated with different concentrations of EC for 24 h. (A) Cell viability was detected by MTT assay. (B, C) Relative reduced GSH and MDA content in L02 cells. (D) Intracellular iron content. (E) GPX4 expression detected by Western Blot. (F) Quantitive analysis of (E). (G) Ferritin expression detected by Western Blot. (H) Quantitive analysis of (G). *$p < 0.05$. EC, ethyl carbamate; GSH, glutathione; MTT, 3-(4,5-dimthyl-2-thiazolyl)-2,5-diphenyl-2-H-tetrazolium bromide; MDA, malondialdehyde; GPX4, glutathione peroxidase 4.

follows: Anti-GPX4 (Abways, CY6959, 1:1500), Anti-Ferritin (Abcam, ab75973, 1:2000), Anti-SLC7A11 (Abcam, ab175186, 1:2000), Anti-Nrf2 for L02 cells (Abcam, ab62352, 1:1000), Anti-Nrf2 for liver tissues (Abclonal, A11159, 1:1000), Anti-pNrf2 (Abcam, ab76026, 1:2000), Anti-GCLC (Abcam, ab20777, 1:1000), Anti-HO-1 (Abcam, ab189491, 1:1000), Anti-NQO1 (Abcam, 1:2000, ab28947), Anti-GAPDH (Abcam, ab181602, 1:10000). Then the membranes were washed with PBST for 3 times and incubated with Anti-rabbit and Anti-mouse IgG HPR-linked secondary antibodies for 1 h, followed by chemiluminescence detection using ChemiDocTM Touch Imaging System (BIO-RAD, California, USA).

2.9. Hematoxylin and eosin (H&E) staining

Liver tissues were fixed in 4% paraformaldehyde for 24 h and dehydrated by a concentration gradient of ethanol solutions, followed by paraffin embedding. Tissue sections were cut, de-waxed, rehydrated, and then stained with hematoxylin and eosin. Then these sections were subjected to microscope analysis.

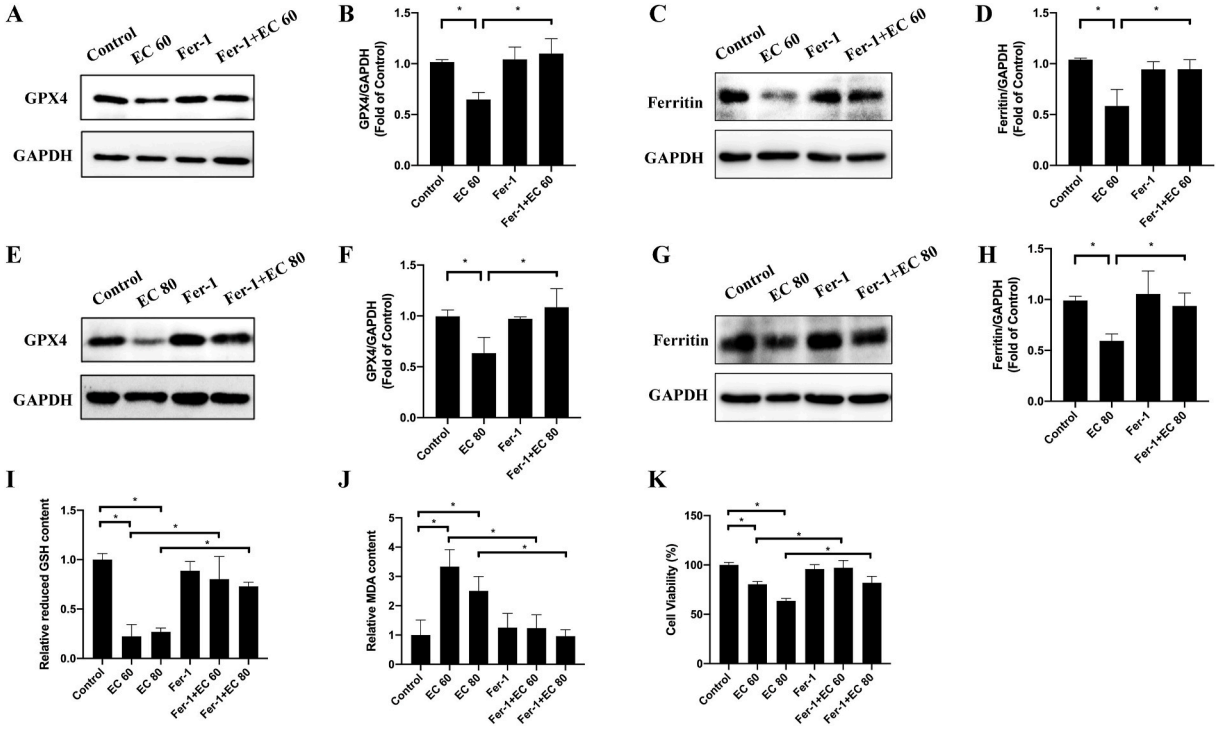

Fig. 2. Inhibition of ferroptosis alleviated EC-induced cell death. L02 cells were first treated with 5 μM Fer-1 for 1 h, and then incubated with 60 mM or 80 mM EC for 24 h. (A, E) Protein levels of GPX4 detected by Western Blot. (B) and (F) Quantitive analysis of (A) and (E). (C, G) Protein levels of Ferritin detected by Western Blot. (D) and (H) Quantitive analysis of (C) and (G). (I, J) Relative reduced GSH and MDA content in L02 cells. (K) Cell viability detected by MTT assay. *$p < 0.05$. EC, ethyl carbamate; Fer-1, ferrostatin-1; GSH, glutathione; MTT, 3-(4,5-dimthyl-2-thiazolyl)-2,5-diphenyl-2-H-tetrazolium bromide; MDA, malondialdehyde; GPX4, glutathione peroxidase 4.

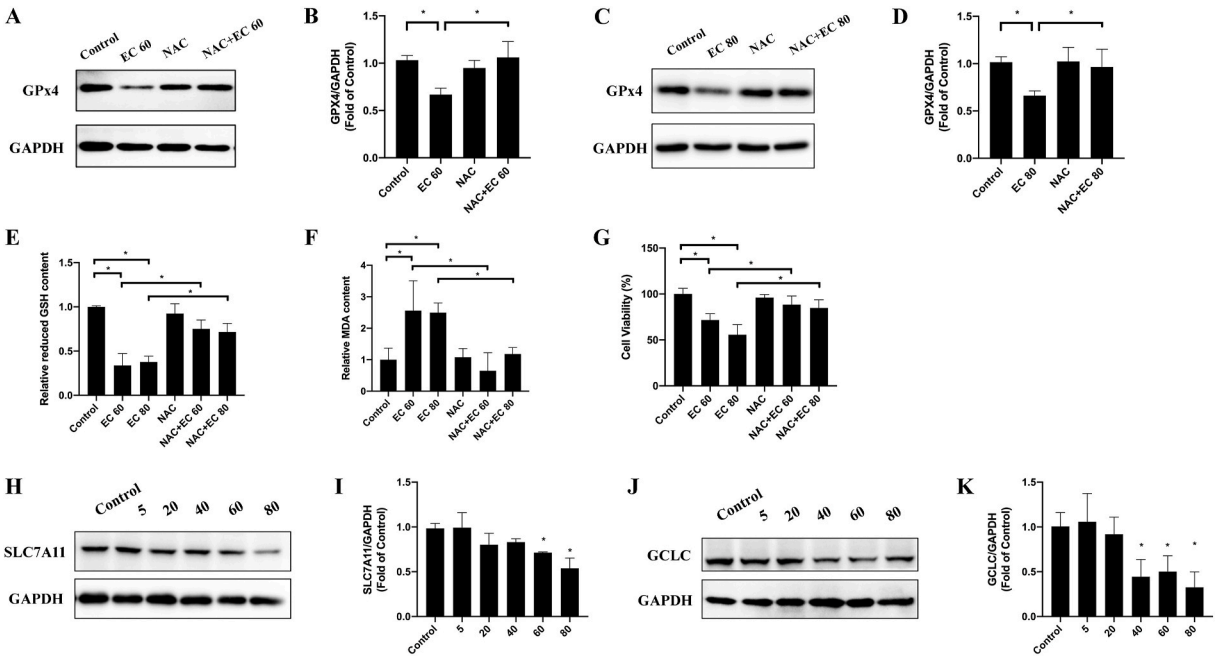

Fig. 3. EC exposure blocked GSH synthesis-related pathways. L02 cells were first treated with 2 mM NAC for 1 h, and then incubated with 60 mM or 80 mM EC for 24 h. (A, C) Protein levels of GPX4 detected by Western Blot. (B) and (D) Quantitative analysis of (A) and (C). (E, F) Relative reduced GSH and MDA content in L02 cells. (G) Cell viability detected by MTT assay. (H, J) SLC7A11 and GCLC expressions detected by Western Blot. (I) and (K) Quantitative analysis of (H) and (J). *$p <$ 0.05. EC, ethyl carbamate; GSH, glutathione; MTT, 3-(4,5-dimthyl-2-thiazolyl)-2,5-diphenyl-2-H-tetrazolium bromide; MDA, malondialdehyde; GPX4, glutathione peroxidase 4; SLC7A11, solute carrier family 7 member 11; GLCL, glutamate cysteine ligase catalytic subunit.

2.10. Immunohistochemistry staining

Immunohistochemistry staining were performed according previous studies [14,28]. Livers were paraffin-embedded and cut into 5 μM-thick sections. After that, these sections were dewaxed and rehydrated, followed by heat-induced epitope retrieval. Subsequently, sections were placed into hydrogen peroxide solution in order to suppress endogenous peroxidase activity. Then the sections were washed with PBS for three times and blocked by BSA solution. Immunohistochemical staining was conducted by incubating primary antibodies for 24 h overnight at 4 °C and then secondary antibodies for 1 h at room temperature. The primary antibodies used for EC toxicity animal experiments were shown as follows: Anti-TNFα (Abways, CY5992, 1:200), Anti-IL-1β (Servicebio, GB11113, 1:200), Anti-NLRP3 (Abways, CY5651, 1:200), Anti-4-HNE (Bioss, bs-10802R, 1:300). The primary antibodies used for Fer-1 and tBHQ rescue experiments were shown as follows: TNFa (Proteintech, 26405-1-AP, 1:200), NLRP3 (Proteintech, 19771-1-AP, 1:200), IL-1β (Servicebio, GB11113, 1:800), 4-HNE (Bioss, bs-6313R, 1:200). Sections were stained with freshly prepared DAB and hematoxylin, then dehydrated and sealed with neutral gum. Images were detected using a Nikon microscope.

2.11. Statistical analysis

Statistical analysis was conducted using Prism 8.0 (GraphPad, USA). Values were expressed as mean ± S.D of at least three independent experiments. The normality and the homogeneity of variance was checked by Shapiro-Wilk tests prior to apply Student's t-test and one-way ANOVA analysis. Student's t-test was used to compare data between two groups, while one-way ANOVA analysis was used for comparison between multiple groups. The boxes and error bars in the figures represent mean value and standard deviation, respectively. Statistical significance was detected if p values < 0.05.

3. Results

3.1. Ethyl carbamate triggered ferroptosis in L02 cells

Ferroptosis is a newly described form of regulated cell death characterized by lipid peroxidation of membranes, intracellular iron accumulation and GSH depletion-induced decreases in GPX4 expression. Based on previous studies [9,26], EC exposure significantly induced ROS overproduction and decline in reduced GSH level, which lead to a hypothesis that EC may trigger ferroptosis in L02 cells. Therefore, we first detected cell viability after treatment with different concentrations of EC for 24 h. According to MTT assay, EC could promote cell death in a dose-dependent fashion (Fig. 1A). Subsequently, we found that EC exposure with concentrations of 60 and 80 mM decreased concentrations of reduced GSH and augmented one of the final products of excess lipid oxidation malondialdehyde (MDA) compared with the control (Fig. 1B and C). Meanwhile, iron contents of EC-treated groups were also elevated (Fig. 1D). Besides, we also determined the protein expression of GPX4 and Ferritin in L02 cells, which are closely related to lipid peroxidation. Compared with the control group, GPX4 and Ferritin expressions both dramatically decreased after EC treatment (Fig. 1E–H). Collectively, our results suggested that EC treatment caused ferroptosis in liver cells.

3.2. Inhibition of ferroptosis alleviated EC-induced cell death

We further investigated the role of ferroptosis in cell death caused by EC exposure. Ferrostain-1 (Fer-1) was recognized as an effective inhibitor of ferroptosis *via* promotion of cystine import and GSH production [29]. A recent study also suggested that Fer-1 could restore Ferritin protein expression in HK-2 cells and diabetic mice [14]. As shown in Fig. 2A–D, compared with 60 mM EC-treated group, Fer-1 pretreatment significantly increased protein expressions of GPX4 and Ferritin. In addition, decreased GPX4 and Ferritin expressions in 80 mM EC-treated group were also recovered by Fer-1 (Fig. 2E and H). In particular, Fer-1 pretreatment increased reduced GSH levels and inhibit up-regulation of

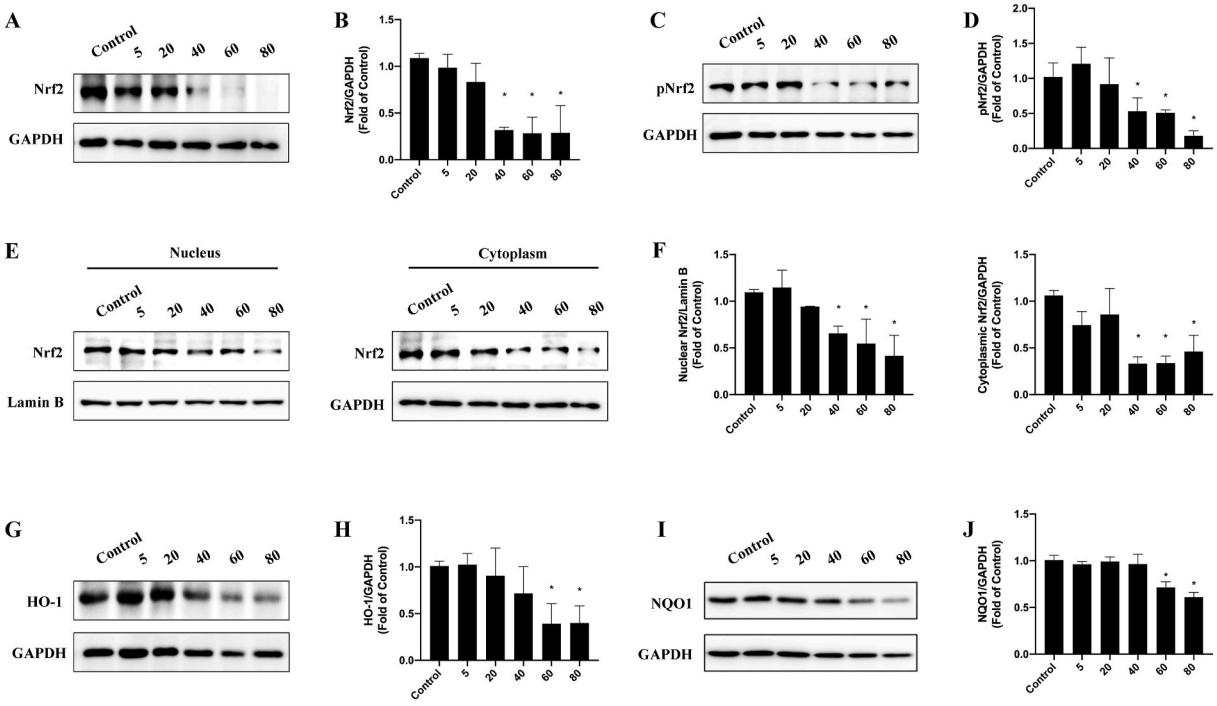

Fig. 4. EC down-regulated Nrf2 pathway. L02 cells were subjected to different concentrations of EC treatment for 24 h. (A, C) Nrf2 and pNrf2 expressions were detected by Western Blot. (B) and (D) Quantitive analysis of (A) and (C). (E) Protein levels of Nrf2 in nucleus and cytoplasm detected by Western Blot. (F) Quantitive analysis of (E). (G, I) HO-1 and NQO1 expressions detected by Western Blot. (H) and (J) Quantitive analysis of (G) and (I). $*p < 0.05$. EC, ethyl carbamate; Nrf2, nuclear factor erythroid 2 related factor 2; HO-1, heme oxygenase-1; NQO1, NAD(P)H quinone oxidoreductase-1.

MDA contents in EC-treated cells (Fig. 2I and J). Additionally, MTT results indicated that Fer-1 treatment could obviously alleviated EC-caused toxicity (Fig. 2K). Taken together, these data suggested that ferroptosis specific inhibitor Fer-1 could reverse ferroptosis-related changes in EC-treated L02 cells, which further implied that ferroptosis was a crucial form of EC-induced cell death.

3.3. EC exposure blocked GSH synthesis-related pathways

GPX4 functions as the major phospholipid hydroperoxides-neutralizing enzyme and its expression and activity mainly depend on Se and GSH levels [24,30]. GSH depletion-induced GPX4 inactivation contribute to ferroptosis caused by ROS overproduction from lipid peroxidation [30]. We, thus, believed that GSH-related pathways might possess critical roles in ferroptosis under EC exposure. *N*-acetyl cysteine (NAC) is a precursor amino acid of GSH biosynthesis. As shown in Fig. 3A–D, NAC pretreatment dramatically increased GPX4 levels compared with EC group, which was consistent with previous study [21]. Notably, we also found that NAC restored reduced GSH contents and MDA levels in EC-treated L02 cells (Fig. 3E–F). As manifested in Fig. 3G, NAC pretreatment also rescued cell death under EC exposure. Together, these results indicated that intracellular GSH depletion might be the main cause of EC-induced ferroptotic cell death.

To further investigate the underlying mechanisms of EC-triggered GSH depletion, we tested two critical proteins SLC7A11 and GCLC for GSH biosynthesis after different concentrations of EC treatment. The amino acid antiporter solute carrier family 7 member 11 (SLC7A11), also commonly known as xCT, maintains GSH generation through importing extracellular cystine and exporting intracellular glutamate [24]. As depicted in Fig. 3H and I, western blotting results showed that EC treatment significantly suppressed SLC7A11 levels compared with the control. Besides, the first step of GSH synthesis depends on conjunction of glutamate and cysteine catalyzed by glutamate cysteine ligase catalytic subunit (GCLC) [31]. As we expected, EC treatment with concentrations of 40, 60 and 80 mM significantly inhibited GCLC expression (Fig. 3J–K). Therefore, these results indicated that EC exposure blocked GSH synthesis-related pathways.

3.4. EC down-regulated Nrf2 pathway

The transcriptional factor nuclear factor erythroid 2 (NFE2)-related factor 2 (Nrf2), the central regulator of antioxidant response, maintains cellular redox balance and also modulates iron storage by regulating relative genes [25,32]. To investigate the underlying mechanism of EC-induced ferroptosis, we tested changes of Nrf2 pathway in EC-treated L02 cells. The western blotting showed that 40, 60 and 80 mM EC treatment markedly decreased total Nrf2 expressions (Fig. 4A–B). Phosphorylation of Nrf2 at Ser-40 through the PKC-based regulation serves as a crucial role in post-translational modification of Nrf2 and dissociation of Nrf2 from Keap1, which may lead to translocation of Nrf2 from cytoplasm to nucleus and activate expressions of target genes [33,34]. As shown in Fig. 4C–D, EC treatment with concentrations of 40, 60 and 80 mM suppressed phosphorylation of Nrf2. We further detected the distribution of Nrf2 in EC-treated cells. The protein expression of Nrf2 in nucleus was notably reduced by EC treatment and Nrf2 in cytoplasm displayed parallel results as nucleus (Fig. 4E–F). In order to further confirm EC-induced changes in Nrf2 signaling pathway, we also determine levels of NAD(P)H quinone oxidoreductase-1 (NQO1) and heme oxygenase-1 (HO-1), downstream related genes of Nrf2. High concentrations (60 and 80 mM) of EC effectively inhibited protein expression of NQO1 and HO-1 (Fig. 4G–J). Given the above results, EC exposure repressed Nrf2 bioactivity and further initiated ferroptosis occurrence.

3.5. Activation of Nrf2 suppressed EC-induced ferroptosis

Tertiary butylhydroquinone (tBHQ), a specific activator of Nrf2, was further used to detected the relationship between Nrf2 and ferroptosis in EC-treated cells. L02 cells were first treated with 10 μM tBHQ for 1 h, followed by incubation with 80 mM EC for 24 h. In accordance with previous studies [35,36], tBHQ pretreatment significantly increased

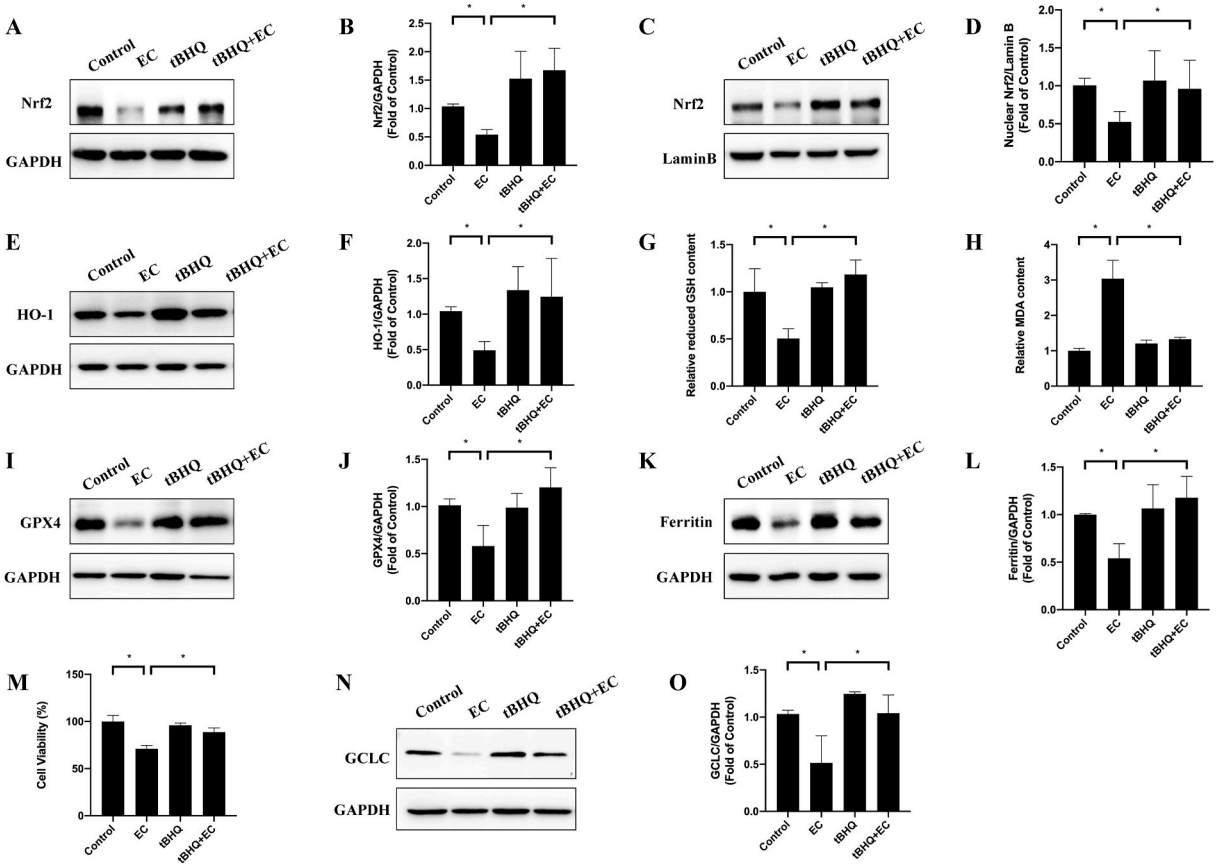

Fig. 5. Nrf2 activation suppressed EC-induced ferroptosis. L02 cells were treated with 10 μM tBHQ for 1 h, followed by incubation with 80 mM EC for 24 h. (A, C) total Nrf2 and nuclear Nrf2 expressions were detected by Western Blot. (B) and (D) Quantitive analysis of (A) and (C). (E) HO-1 expressions detected by Western Blot. (F) Quantitive analysis of (E). (G, H) Relative reduced GSH and MDA content in L02 cells. (I, K) GPX4 and Ferritin protein expressions. (J) and (L) Quantitive analysis of (I) and (K). (M). Cell viability was detected by MTT assay. (N) GCLC protein expression. (O) Quantitive analysis of (N). EC, ethyl carbamate; tBHQ, tert-butylhydroquinone; GSH, glutathione; MTT, 3-(4,5-dimthyl-2-thiazolyl)-2,5-diphenyl-2-H-tetrazolium bromide; MDA, malondialdehyde; GPX4, glutathione peroxidase 4; Nrf2, nuclear factor erythroid 2 related factor 2; HO-1, heme oxygenase-1; GLCL, glutamate cysteine ligase catalytic subunit.

total and nuclear expressions of Nrf2 (Fig. 5A–D), as well as Nrf2 downstream factor HO-1 level (Fig. 5E and F), which indicated the activation of Nrf2 by tBHQ in EC-treated L02 cells. Furthermore, tBHQ notably inhibited MDA upregulation and enhanced reduced GSH level under EC exposure (Fig. 5G and H). The protein expressions of GPX4 and Ferritin were significantly reversed by tBHQ pretreatment (Fig. 5I–L). MTT assay revealed that tBHQ alleviated EC-induced cell death in Fig. 5M. Besides, tBHQ augmented expression of GSH biogenesis critical protein GCLC (Fig. 5N and O). These results suggested that Nrf2 activation by tBHQ successfully blocked EC-induced ferroptosis and elevated GSH level. Therefore, Nrf2 inactivation played a central role in EC-induced ferroptosis.

3.6. EC caused liver dysfunction and inflammation in vivo

To elucidate EC-induced toxicity *in vivo*, Balb/c mice were continuously administrated with EC for 28 days. As depicted in Fig. 6A and B, 450 mg/kg EC notably decreased body weight from the second week. As shown in Fig. 6C, 450 mg/kg EC significantly decreased liver index, which is consistent with changes of body weight. Although 150 mg/kg EC failed to affect body weight, liver index of 150 mg/kg group slightly decreased compared with control group. Results of H&E staining showed that EC caused inflammatory cell infiltration near the central vein (Fig. 6D). Moreover, serum aspartate aminotransferase (AST) and alanine aminotransferase (ALT) activities in EC group were notably increased (Fig. 6E–F), which indicated that EC treatment presented negative effects of functional damage in liver. Taken together, these results suggested that EC administration triggered serve liver dysfunction *in vivo*.

EC has been reported to elevated inflammatory cytokines IL-1β and IL-6 expression as well as inflammation-related NF-κB signaling in lung [37,38]. We, thus, determined whether EC treatment leads to hepatic inflammation in liver. NLRP3, IL-1β and TNFα protein expressions were tested by immunohistochemical staining assay. The NLRP3 inflammasome, a multimeric cytosolic protein complex, is produced in response to damage-associated molecular patterns and pathogen-associated molecular patterns under cellular perturbation, and is detrimental in many inflammation-related human diseases [39]. We found that EC treatment were significantly up-regulated levels of NLRP3 (Fig. 6G–H). NLRP3 initiates maturation and release of pro-inflammatory cytokines IL-1β by activation caspase 1 [39]. IL-1β expression was also apparently increased in EC-exposed group (Fig. 6I–J), which was consistent with changes in NLRP3 levels. In addition, inflammation is also characterized by activation of immune cells and generation of tumor necrosis factor alpha (TNFα) [40]. EC administration also enhanced expressions of TNFα, compared with the control (Fig. 6K–L). According to the above results, EC treatment promoted severe inflammation in liver.

3.7. EC triggered oxidative stress in liver

Since EC-initiated ROS overproduction was detected in liver cells [9,26], we speculated that EC administration might lead to oxidative stress *in vivo*. Superoxide dismutase (SOD) protects biological systems against high chemical reactivity of ROS or RNS under redox imbalance [41]. As

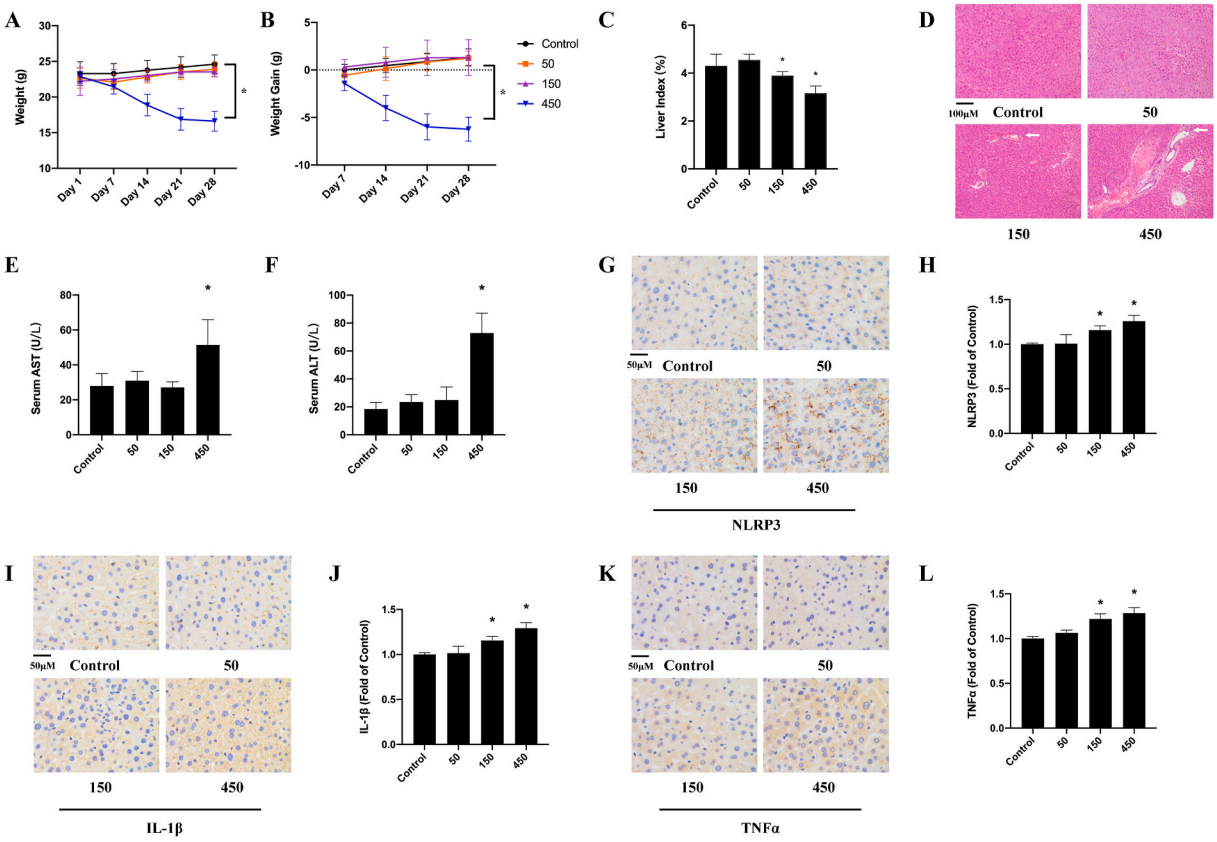

Fig. 6. EC caused liver dysfunction and inflammation *in vivo*. (A, B) Body weight and body weight gain in EC-treated Balb/c mice. (C) Liver index. (E) Morphology of liver tissues by H&E staining. The white arrow manifest inflammatory cell infiltration. (F, H) AST and ALT levels in serum were detected by commercial kits. (G, I and K) NLRP3, IL-1β and TNFα expressions were detected by immunohistochemical staining. (H, J and L) Quantitive analysis of (G, I and K). *$p < 0.05$. EC, ethyl carbamate; H&E staining, hematoxylin and eosin staining; AST, aspartate aminotransferase; ALT, alanine aminotransferase. EC, ethyl carbamate; NLRP3, NOD-, LRR- and pyrin domain-containing protein 3; IL-1β, interleukin-1β; TNFα, tumor necrosis factor alpha.

depicted in Fig. 7A, EC significantly decreased SOD activity in liver. Furthermore, GSH contents were also dramatically dropped after EC treatment (Fig. 7B), which indicated that EC treatment caused redox disturbance *in vivo*. Redox imbalance may lead to oxidation of protein, lipid and other essential biological macromolecules. Therefore, we focused on determination of lipid peroxidation by detecting end-products 4-hydroxynonenal (4HNE) and MDA. As expected, MDA in liver and serum was also increased notably by EC administration (Fig. 7C–D). EC augmented levels of another final product of lipid peroxidation 4HNE according to immunohistochemical staining assay (Fig. 7E–F). Collectively, these results denoted that EC treatment could lead to redox imbalance, especially lipid peroxidation in liver.

3.8. EC enhanced ferroptosis and suppressed Nrf2 and GSH synthesis-related proteins in vivo

Based on results of GSH depletion and elevation of lipid peroxidation, we hypothesized that EC might induce ferroptosis in liver. As manifested in Fig. 8A and B, the concentrations of iron in liver and serum were obviously increased by EC administration. Then we detected ferroptosis hallmarks GPX4 and Ferritin. Results of western blot showed that GPX4 and Ferritin of EC groups were remarkedly suppressed compared with the control (Fig. 8C–F), which were consistent with EC-treated L02 cells. The ultrastructural analysis indicated damaged mitochondria membrane and ridge reduction or absence in EC-exposed group, as well as total mitochondria swelling, which probably marked the initiation of ferroptosis (Fig. 8G). The above results implied that EC promoted ferroptosis in liver.

SLC7A11, the key component of cystine/glutamate antiporter, promotes GSH synthesis by increasing intracellular cystine contents. As shown in Fig. 8H and I, 450 mg/kg EC administration repressed SLC7A11 expression, while 50 and 150 mg/kg EC failed to affect SLC7A11 levels. Besides, we also detected changes in another GSH synthesis-related protein GCLC by EC exposure. Notably, EC also decreased GCLC expressions compared with the control (Fig. 8J and K). EC-induced reduction in expressions of SLC7A11 and GCLC *in vivo* were consistent with results in EC-exposed L02 cells. SLC7A11 and GCLC were downstream elements of Nrf2 signaling, which acts as a central role in response to oxidative stress and regulation of ferroptosis process. The western blotting results showed that EC inhibited Nrf2 expressions, compared with the control (Fig. 8L and 8M). Together, EC decreased Nrf2 levels and blocked GSH generation *in vivo*, which ultimately initiated ferroptosis after EC administration.

3.9. Fer-1 and tBHQ alleviated EC-induced liver injury and inflammation

Since Fer-1 and tBHQ could significantly reverse EC-induced ferroptosis in liver cells, we detected Fer-1 and tBHQ protection in Balb/c mice. As shown in Fig. 9A–B, Fer-1 or tBHQ pretreatment increased body weight and liver index, compared with EC group. Besides, serum AST and ALT levels were decreased remarkably by Fer-1 and tBHQ. In addition, Fer-1 and tBHQ also recovered liver structure disorder by decreasing inflammatory cell infiltration near the central vein according to results of H&E staining (Fig. 9E). Besides, cotreatment of EC with Fer-1 or tBHQ inhibited liver inflammation by detection of decreased expression of IL-1β, NLRP3 and TNFα (Fig. 9F–I). Therefore, Fer-1 and tBHQ improved EC-induced liver injury and inflammation in Balb/c mice, which suggested that inhibition of ferroptosis and Nrf2 activation

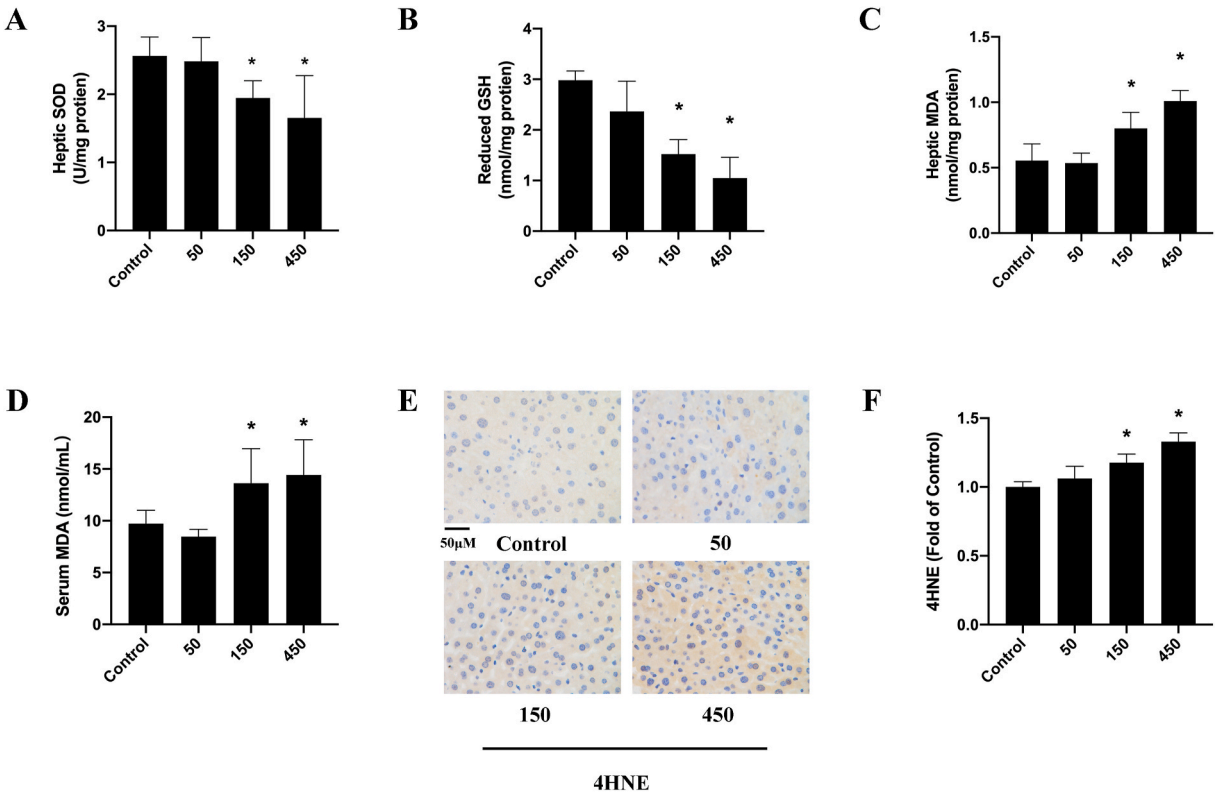

Fig. 7. EC triggered oxidative stress in liver. (A–D) Hepatic SOD activities, hepatic GSH and MDA contents, as well as serum MDA levels were detected using commercial assay kits. (E) 4HNE levels were analyzed by immunohistochemical staining. (F) Quantitive analysis of (E). *$p < 0.05$. EC, ethyl carbamate; GSH, glutathione; MDA, malondialdehyde; 4HNE, 4-hydroxynonenal.

could suppress EC-caused hepatic damage.

3.10. *Fer-1 and tBHQ inhibited EC-caused ferroptosis in vivo*

As a potent inhibitor of ferroptosis, Fer-1 has also been proved to prevent ferroptosis *in vivo* [14]. The increased hepatic iron content and MDA were blocked and decreased levels of reduced GSH were rescued by Fer-1 pretreatment, compared with EC group (Fig. 10A–C). Remarkable decreases in 4HNE level were also observed in Fer-1+EC group (Fig. 10D–E), which implied that Fer-1 protected against lipid peroxidation under EC exposure. Besides, Fer-1 inhibited degradation of GPX4 and Ferritin, compared with EC group (Fig. 10F–I). These above results further illustrated that Fer-1 reversed ferroptosis-related factors caused by EC and ferroptosis might be a critical form of EC-induced liver injury.

In order to investigated the role of Nrf2 in EC-caused ferroptosis *in vivo*, we also detected these indicators in tBHQ+EC group. The western blotting results revealed that tBHQ pretreatment upregulated Nrf2 expression, indicating that tBHQ notably activated Nrf2 in liver (Fig. 11A and B). As depicted in Fig. 10A–E, tBHQ significantly recovered hepatic iron content, reduced GSH level and ameliorated lipid peroxidation, which presented the parallel results with Fer-1. Furthermore, tBHQ pretreatment enhanced GPX4 and Ferritin levels (Fig. 11C–E). Accordingly, tBHQ displayed positive effects on EC-induced ferroptosis in BALB/c mice. We also investigated GSH biogenesis pathway by evaluation of SLC7A11 and GCLC expression. As shown in Fig. 11F–I, tBHQ dramatically inhibited depletion of SLC7A11 and GCLC under EC exposure, which might lead to reduction in GSH generation. Therefore, these results illustrated that Nrf2 deficiency caused by EC enhanced the sensitivity to ferroptosis.

4. Discussion

The present study demonstrated that EC triggered GSH depletion, lipid peroxidation and iron overload, as well as decreased expression of GPX4 and Ferritin, characteristic indicators of ferroptosis. Ferroptosis inhibitor Fer-1 blocked EC-induced cytotoxicity and recovered ferroptosis-associated changes, which further indicated that ferroptotic cell death was critical for declines in cell viability. Mechanistically, EC-initiated ferroptosis was ascribed to disturbed GSH synthesis and inhibition of Nrf2 signaling (Fig. 12).

Despite maintaining cellular functions by regulation of intracellular signaling and redox balance, ROS may lead to oxidative damage of biological macromolecules and organelles [42]. We previously reported that EC exposure triggered ROS overproduction-mediated cytotoxicity in L02 cells [9]. Therefore, the mechanism of hepatic cell dysfunction upon EC exposure might be related to ROS-modulated cell death. Ferroptosis is defined as a ROS-dependent form of cell death and characterized with two main features, iron upload and lipid peroxidation [24]. Interestingly, we found that EC treatment could elevated iron content both in hepatic cells and livers of Balb/c mice. The iron-storage protein ferritin functions as the central regulator in iron-buffering system, which can sequester excess free iron in a protein cage [43]. The expressions of Ferritin decreased after EC exposure *in vivo* and *in vitro*, which contributed to EC-induced excess iron content. Iron overload causes ROS overproduction through a Fenton reaction and further promotes ferroptosis *via* activation of specific downstream elements after lipid ROS generation. Ferroptosis-related lipid peroxidation, driven by reaction of free radicals and polyunsaturated fatty acids existing in biomembranes, produces lipid hydroperoxides (LOOHs) [29,44]. LOOHs are subsequently oxidized to MDA and 4HNE, two common final products of lipid peroxidation. MDA and 4HNE contents increased notably in EC-treated group, which indicated massive lipid peroxidation under EC exposure. Thus, we suggested that EC treatment triggered ferroptosis in L02 cells

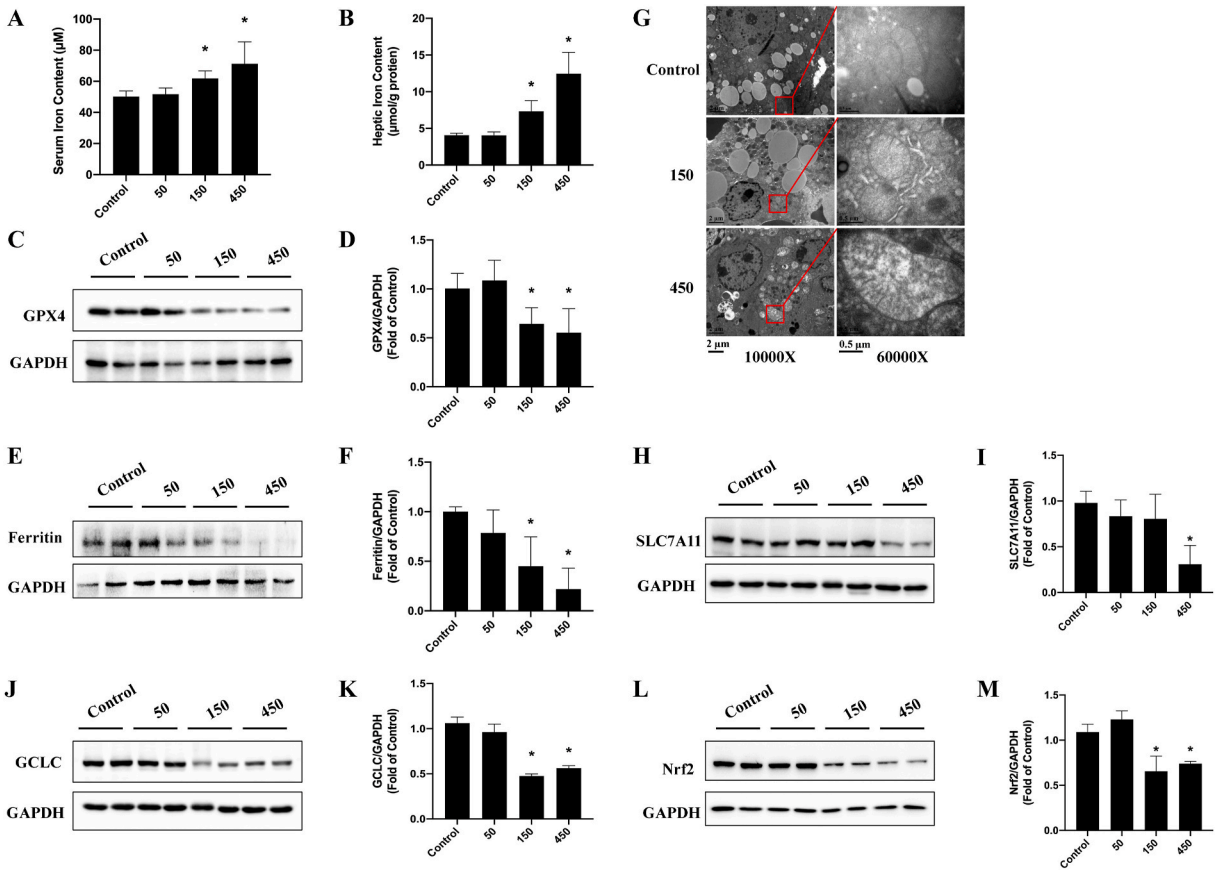

Fig. 8. EC enhanced ferroptosis and suppressed Nrf2 and GSH synthesis-related proteins *in vivo*. (A, B) Iron contents in liver and serum were detected using commercial assay kits. (C, E) GPX4 and Ferritin expressions were determined by Western Blot. (D, F) Quantitive analysis of (C) and (E). (G) TEM analysis of mitochondria. (H, J, L) SLC7A11, GCLC and Nrf2 expressions were detected by Western Blot. (I, K, M) Quantitive analysis of (H), (J) and (L). *$p < 0.05$. EC, ethyl carbamate; GPX4, glutathione peroxidase 4; SLC7A11, solute carrier family 7 member 11; GLCL, glutamate cysteine ligase catalytic subunit; Nrf2, nuclear factor erythroid 2 related factor 2.

and livers of mice. Furthermore, we observed effects on ferroptotic cell death by Fer-1 pretreatment, a commonly used ferroptosis inhibitor. Fer-1 has been reported to effectively inhibit ROS overproduction and lipid peroxidation, which ultimately blocked ferroptosis process [29]. Our results showed that Fer-1 recovered expressions of Ferritin and GPX4, lipid peroxidation and toxicity compared with EC group *in vitro* and *in vivo*, indicating that ferroptosis is a critical contributor to EC-triggered hepatic toxicity.

Mitochondria are the center modulator of energy production and metabolism. Oxidative phosphorylation is the major source of ROS generation. Increasing evidence proves that mitochondria play a vital role in ferroptotic cell death. Many investigators concur that interruption of mitochondrial ROS generation can impede ferroptosis [45,46]. Besides, ferroptotic cells usually display abnormal mitochondria, such as condensation or swelling, decreased or disappeared crista, as well as damaged membrane [13,23,29]. According to TEM analysis, EC exposure caused rupture of mitochondrial membrane and disappearance of crista, indicating the occurrence of mitochondrial dysfunctions and activation of ferroptosis. Apart from ferroptosis, mitochondria are also important organelles for regulation of inflammation. Damaged mitochondria initiate assembly of NLRP3 inflammasomes and further result in caspase-1-dependent secretion of the pro-inflammatory cytokines IL-1β [47,48]. In turn, pro-inflammatory mediators, including TNFα and IL-1β, inhibit mitochondrial respiratory chain complex 1, ATP production, mitochondrial membrane potential and aggravate ROS overproduction [49,50]. Our data indicated EC-induced inflammation by detection of profound increases in NLRP3, IL-1β and TNFα levels, which might be closely associated with mitochondrial abnormalities and dysfunctions.

In Fer-1 rescue experiment, we observed that Fer-1 pretreatment significantly inhibited EC-caused upregulation in NLRP3 expression. A recent study was also showed downregulation by Fer-1 treatment on NLRP3 levels [51], which was consistent with our results. According to previous study, ATP exposure caused significant decreases in GSH levels in macrophages, which further led to NLRP3 inflammasome activation [52]. Besides, pre-treatment with a cell-permeable ethyl-ester form of GSH limited NLRP3 inflammasome activation [53]. GSH is an important cofactor of GPX4 and triggers GSH-mediated reduction of phospholipid hydroperoxides into alcohols, finally inhibiting ROS accumulation and iron-dependent cell death [54]. Promotion of GPX4 expression by compound C possess an inhibitory effect on NLRP3 inflammasome activation [55]. Based on these studies, GPX4-GSH pathway displayed negative regulation of NLRP3. Therefore, increased expression of NLRP3 may be ascribe to inhibition of GPX4-GSH pathway in EC-induced ferroptosis.

GPX4-GSH-cysteine axis is regarded as the key node of ferroptosis *via* modulation of lipid peroxidation [21,23]. GPX4 represses lipid peroxidation by reduction of phospholipid hydroperoxide to corresponding alcohols [56,57]. It is reasonable to assume that EC-induced lipid peroxidation was attribute to suppression of GPX4 levels. The expression and activity of GPX4 are greatly dependent on selenium and GSH [24]. GSH prevents severe damage of ferroptosis by acting as the reducing substrate of GPX4. We observed that NAC, a well-known precursor of GSH, rescued GX4 suppression in EC-treated cells. Hence, inhibition of GPX4 by EC treatment might ascribe to GSH depletion. Not surprising, multiple pathways and complicated processes may alter GSH

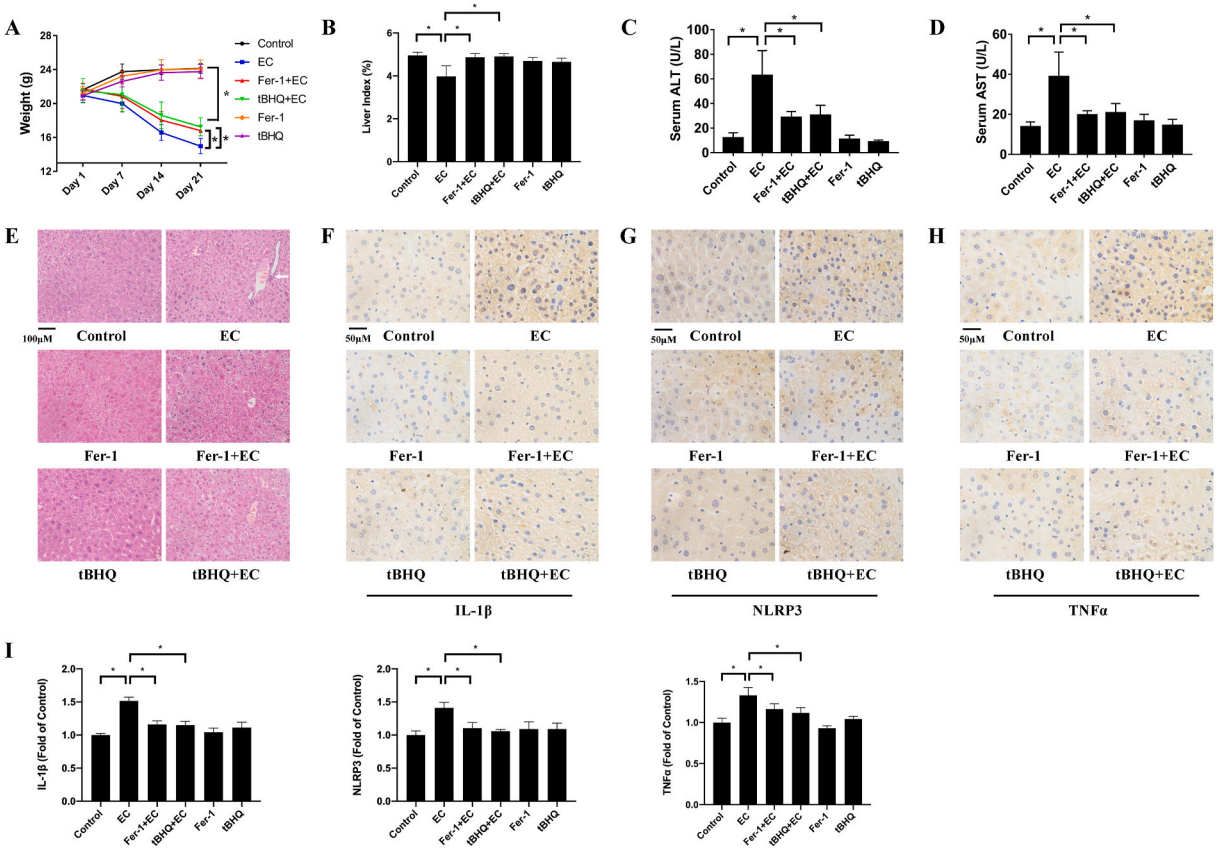

Fig. 9. Fer-1 and tBHQ alleviated EC-induced liver injury and inflammation. (A) Body weight of Balb/c mice. (B) Liver index. (C, D) AST and ALT levels in serum were detected by commercial kits. (E) Morphology of liver tissues by H&E staining. The white arrow manifest inflammatory cell infiltration. (F, G and H) IL-1β, NLRP3 and TNFα expressions were detected by immunohistochemical staining. (I) Quantitive analysis of (G, I and K). $*p < 0.05$. EC, ethyl carbamate; Fer-1, ferrostatin-1; tBHQ, tert-butylhydroquinone; H&E staining, hematoxylin and eosin staining; AST, aspartate aminotransferase; ALT, alanine aminotransferase; NLRP3, NOD-, LRR- and pyrin domain-containing protein 3; IL-1β, interleukin-1β; TNFα, tumor necrosis factor alpha.

concentration. Vinly carbamate epoxide, the final product of EC oxidation catalyzed by cytochrome P450 enzyme, can be conjugated with GSH [58–60]. Besides, GSH can also be eliminated by EC-caused excessive ROS in order to recover intracellular redox imbalance [61]. Furthermore, we also detected changes in GSH synthesis-related SLC7A11 and GCLC *in vitro* and *in vivo*. It is reported that various small-molecule compounds could cause inhibition of SLC7A11 to initiate ferroptosis [29,62]. The amino acid antiporter SLC7A11, also called xCT, is indispensable for GSH synthesis by exchanging intracellular glutamate for extracellular cystine [12,24]. The synthetic rate of GSH is mainly limited by cystine level. Cysteine is generated by its precursor cystine and subsequently formed glutamate-cysteine with glutamate, which depends on activity of glutamate-cysteine ligase (GCL). Treatment with buthionine sulfoximine (BSO), an effective inhibitor of GCL, has been confirmed to up-regulate ferroptosis process [63,64]. The glutamate-cysteine ligase catalytic subunit (GCLC) can control functions of GCL and be responsible for GSH production. Downregulated expressions of SLC7A11 and GCLC were observed in EC-treated L02 cells and liver tissues. These results implied that EC disturbed GSH synthesis and decreased GPX4 level, which further enhanced ferroptotic cell death.

The nuclear factor erythroid 2-realted factor 2 (Nrf2) is one of the main transcription factors of the cellular antioxidant response and serves as a key mediator for ferroptosis. In normal conditions, Nrf2 binds with its negative regulator Keap1, then subjected to ubiquitination and ultimate degradation by the proteasome. Phosphorylated form of Nrf2 can be released from Keap1 and translocated to nucleus, thereby promoting transcription of downstream targeted genes [65]. Initiation of Nrf2 activity enhances GSH synthesis by up-regulating SLC7A11 and GCLC expressions. Antioxidant system, meanwhile, can be strengthened by Nrf2-triggered heme oxygenase 1(HO-1) and NAD(P)H quinone oxidoreductase-1 (NQO1). We found obvious decreases in nuclear Nrf2 and pNrf2, as well as Nrf2-targeted SLC7A11, GCLC, HO-1 and NQO1 in EC-exposed group, indicating that EC treatment resulted in Nrf2 inactivation. Additionally, Nrf2 signaling also possesses regulatory role in iron metabolism. Ferritin protein mainly consists of ferritin heavy chain (FTH1) and ferritin light chain (FTL) polypeptides [66]. Deficiency of Nrf2 induced apparently lower mRNA levels of *Fth1* and *Ftl* [67,68], whereas dithiolethiones, known as potent Nrf2 activators, increased *Fth1* and *Ftl* transcription by regulation of Nrf2 signaling [69]. Besides, gel shift assay also proved that Nrf2 could directly bind to *Fth1* [69]. Therefore, we suggested that EC-induced Nrf2 inactivation alters iron homeostasis by decreasing Ferritin and iron storage, which further triggered occurrence of ferroptosis. tBHQ, regarded as a specific Nrf2 activator, can effectively prevent ferroptosis by decreasing iron content and inhibiting lipid peroxidation [70]. In this study, tBHQ also exert positive impacts on EC-caused ferroptosis in liver cells and Balb/c mice. Additionally, tBHQ stimulated Nrf2-regulated GSH generation pathway by upregulating related proteins expression. Therefore, suppression of Nrf2 increased ferroptosis sensitivity of L02 cells and liver under EC exposure.

In conclusion, our study for the first time revealed that EC treatment resulted in ferroptosis as a critical form of cell death, which was identified by iron accumulation and lipid peroxidation. Suppressed GPX4 by GSH depletion and Nrf2 inactivation were of great significance in promoting progression of EC-induced ferroptosis. Hence, we provided a novel insight into the underlying mechanisms and raised health concern of EC-induced toxicity.

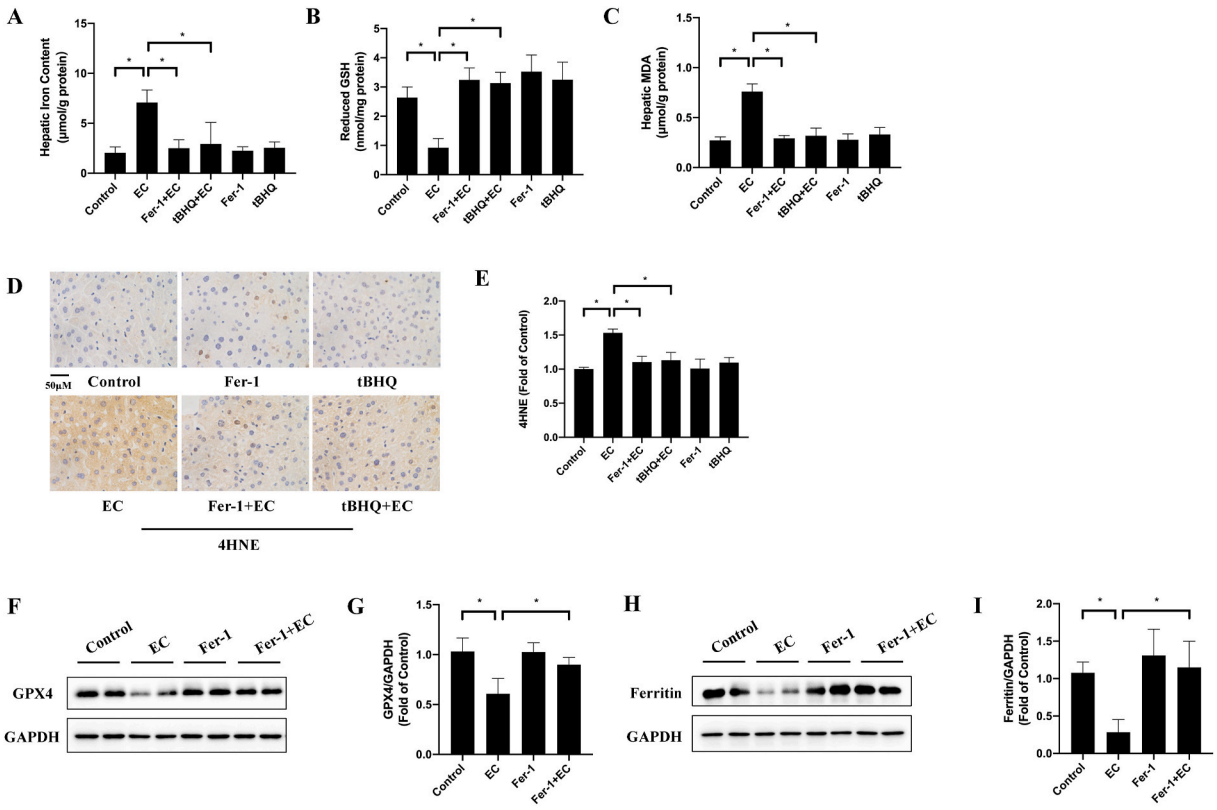

Fig. 10. Fer-1 and tBHQ inhibited iron content and lipid peroxidation. (A–C) Iron contents, reduced GSH and MDA in liver were detected using commercial assay kits. (D) 4HNE levels were detected by immunohistochemical staining. (E) Quantitive analysis of (D). (F, H) GPX4 and Ferritin expressions were determined by Western Blot. (G, I) Quantitive analysis of (F) and (H). $*p < 0.05$. EC, ethyl carbamate; Fer-1, ferrostatin-1; tBHQ, tert-butylhydroquinone; 4HNE, 4-hydroxynonenal.

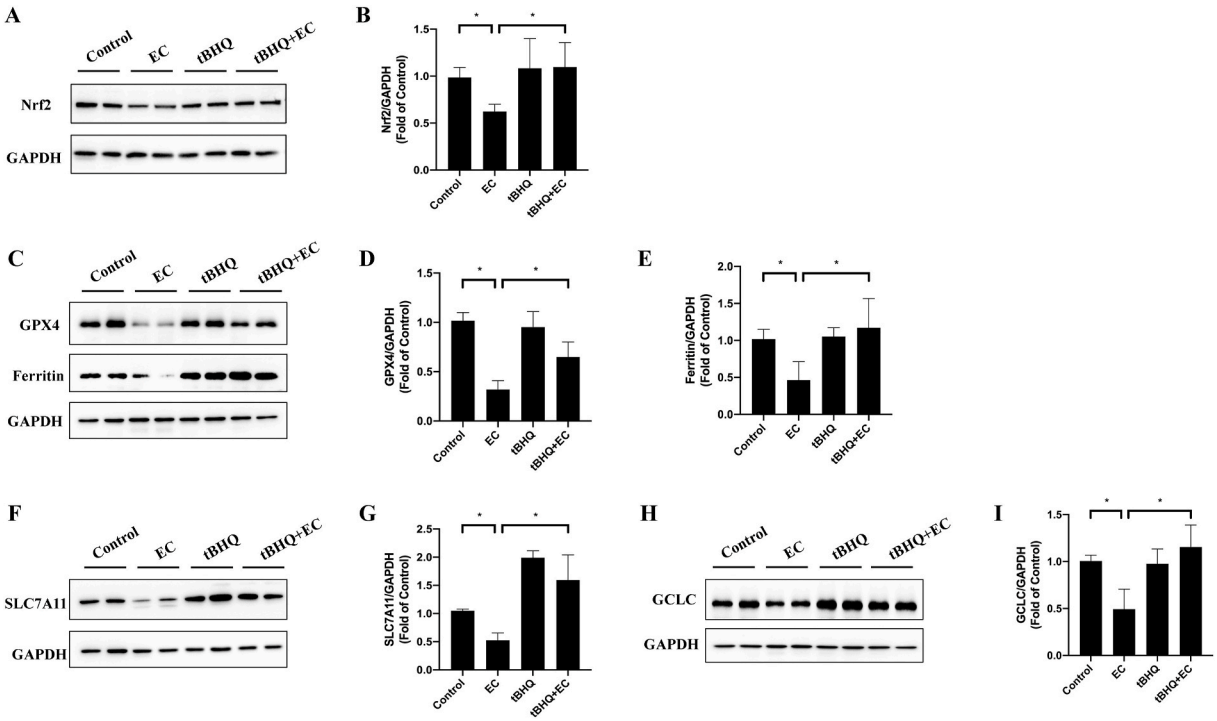

Fig. 11. tBHQ increased Nrf2 and GSH synthesis-related proteins *in vivo*. (A, C, F and H) Nrf2, GPX4, Ferritin, SLC7A11 and GCLC expressions were determined by Western Blot. (B, D, E, G and I) Quantitive analysis of (A), (C), (F) and (H). $*p < 0.05$. EC, ethyl carbamate; tBHQ, tert-butylhydroquinone. GPX4, glutathione peroxidase 4; SLC7A11, solute carrier family 7 member 11; GLCL, glutamate cysteine ligase catalytic subunit; Nrf2, nuclear factor erythroid 2 related factor 2.

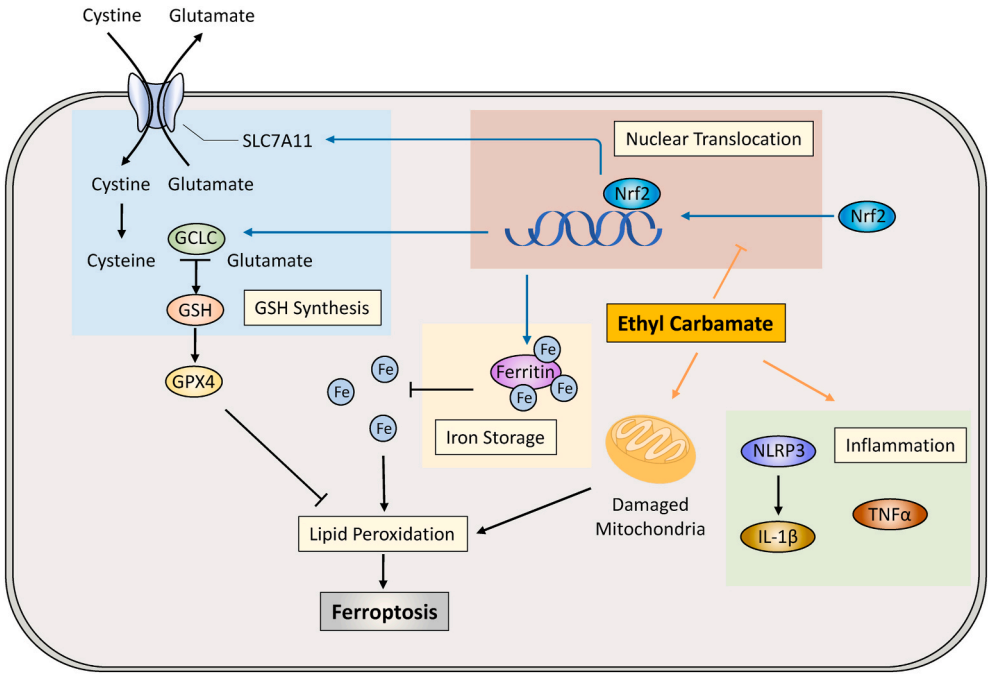

Fig. 12. Schematic diagram for EC-induced ferroptosis.

Declaration of competing interest

The authors declare no conflict of interests.

Acknowledgements

This work was supported by National Natural Science Foundation of China (21876152), Zhejiang Provincial Natural Science Foundation of China (LR18C200002), National Postdoctoral Program for Innovative Talents (BX20190296) and China Postdoctoral Science Foundation (2019M662065).

References

[1] S. Jung, S. Kim, M. Chung, B. Moon, S. Shin, J. Lee, Risk assessment of ethyl carbamate in alcoholic beverages in Korea using the margin of exposure approach and cancer risk assessment, Food Control 124 (2021), https://doi.org/10.1016/j.foodcont.2021.107867.

[2] V. Gowd, H. Su, P. Karlovsky, W. Chen, Ethyl carbamate: an emerging food and environmental toxicant, Food Chem. 248 (2018) 312–321, https://doi.org/10.1016/j.foodchem.2017.12.072.

[3] P. Hübner, P.M. Groux, B. Weibel, C. Sengstag, J. Horlbeck, P. Leong-Morgenthaler, J. Lüthy, Genotoxicity of ethyl carbamate (urethane) in Salmonella, yeast and human lymphoblastoid cells, Mutat. Res. 390 (1997) 11–19, https://doi.org/10.1016/S0165-1218(96)00160-7.

[4] D. Balli, Y. Zhang, J. Snyder, V.V. Kalinichenko, T.V. Kalin, Endothelial cell-specific deletion of transcription factor FoxM1 increases urethane-induced lung carcinogenesis, Cancer Res. 71 (2011) 40–50, https://doi.org/10.1158/0008-5472.CAN-10-2004.

[5] F.A. Beland, R.W. Benson, P.W. Mellick, R.M. Kovatch, D.W. Roberts, J.L. Fang, D. R. Doerge, Effect of ethanol on the tumorigenicity of urethane (ethyl carbamate) in B6C3F1 mice, Food Chem. Toxicol. 43 (2005) 1–19, https://doi.org/10.1016/j.fct.2004.07.018.

[6] S.H. Chun, Y.N. Cha, C. Kim, Urethane increases reactive oxygen species and activates extracellular signal-regulated kinase in RAW 264.7 macrophages and A549 lung epithelial cells, Arch Pharm. Res. (Seoul) 36 (2013) 775–782, https://doi.org/10.1007/s12272-013-0104-8.

[7] W. Chen, Y. Xu, L. Zhang, H. Su, X. Zheng, Blackberry subjected to in vitro gastrointestinal digestion affords protection against Ethyl Carbamate-induced cytotoxicity, Food Chem. 212 (2016) 620–627, https://doi.org/10.1016/j.foodchem.2016.06.031.

[8] W. Chen, Y. Xu, L. Zhang, Y. Li, X. Zheng, Wild raspberry subjected to simulated gastrointestinal digestion improves the protective capacity against ethyl carbamate-induced oxidative damage in caco-2 cells, Oxid. Med. Cell. Longev. (2016) 3297363, https://doi.org/10.1155/2016/3297363, 2016.

[9] Y. Li, X. Ye, X. Zheng, W. Chen, Transcription factor EB (TFEB)-mediated autophagy protects against ethyl carbamate-induced cytotoxicity, J. Hazard Mater. 364 (2019) 281–292, https://doi.org/10.1016/j.jhazmat.2018.10.037.

[10] B. D'Autreaux, M.B. Toledano, ROS as signalling molecules: mechanisms that generate specificity in ROS homeostasis, Nat. Rev. Mol. Cell Biol. 8 (2007) 813–824, https://doi.org/10.1038/nrm2256.

[11] H. Sies, D.P. Jones, Reactive oxygen species (ROS) as pleiotropic physiological signalling agents, Nat. Rev. Mol. Cell Biol. 21 (2020) 363–383, https://doi.org/10.1038/s41580-020-0230-3.

[12] Y. Xie, W. Hou, X. Song, Y. Yu, J. Huang, X. Sun, R. Kang, D. Tang, Ferroptosis: process and function, Cell Death Differ. 23 (2016) 369–379, https://doi.org/10.1038/cdd.2015.158.

[13] X. Chen, R. Kang, G. Kroemer, D. Tang, Organelle-specific regulation of ferroptosis, Cell Death Differ. 28 (2021) 2843–2856, https://doi.org/10.1038/s41418-021-00859-z.

[14] S. Li, L. Zheng, J. Zhang, X. Liu, Z. Wu, Inhibition of ferroptosis by up-regulating Nrf2 delayed the progression of diabetic nephropathy, Free Radic. Biol. Med. 162 (2020) 435–449, https://doi.org/10.1016/j.freeradbiomed.2020.10.323.

[15] X. Yao, W. Li, Fang, C. Xiao, X. Wu, M. Li, Z. Luo, Emerging roles of energy metabolism in ferroptosis regulation of tumor cells, Adv. Sci. (2021), e2100997, https://doi.org/10.1002/advs.202100997.

[16] S. David, P. Jhelum, F. Ryan, S.Y. Jeong, A. Kroner, Dysregulation of iron homeostasis in the CNS and the role of ferroptosis in neurodegenerative disorders, Antioxid Redox Signal (2021), https://doi.org/10.1089/ars.2021.0218.

[17] K. Vats, O. Kruglov, A. Mizes, S.N. Samovich, A.A. Amoscato, V.A. Tyurin, Y. Y. Tyurina, V.E. Kagan, Y.L. Bunimovich, Keratinocyte death by ferroptosis initiates skin inflammation after UVB exposure, Redox Biol. 47 (2021) 102143, https://doi.org/10.1016/j.redox.2021.102143.

[18] S. Wei, T. Qiu, X. Yao, N. Wang, L. Jiang, X. Jia, Y. Tao, Z. Wang, P. Pei, J. Zhang, Y. Zhu, G. Yang, X. Liu, S. Liu, X. Sun, Arsenic induces pancreatic dysfunction and ferroptosis via mitochondrial ROS-autophagy-lysosomal pathway, J. Hazard Mater. 384 (2020) 121390, https://doi.org/10.1016/j.jhazmat.2019.121390.

[19] X. Qin, J. Zhang, B. Wang, G. Xu, X. Yang, Z. Zou, C. Yu, Ferritinophagy is involved in the zinc oxide nanoparticles-induced ferroptosis of vascular endothelial cells, Autophagy (2021) 1–20, https://doi.org/10.1080/15548627.2021.1911016.

[20] M. Yoshida, S. Minagawa, J. Araya, T. Sakamoto, H. Hara, K. Tsubouchi, Y. Hosaka, A. Ichikawa, N. Saito, T. Kadota, N. Sato, Y. Kurita, K. Kobayashi, S. Ito, H. Utsumi, H. Wakui, T. Numata, Y. Kaneko, S. Mori, H. Asano, M. Yamashita, M. Odaka, T. Morikawa, K. Nakayama, T. Iwamoto, H. Imai, K. Kuwano, Involvement of cigarette smoke-induced epithelial cell ferroptosis in COPD pathogenesis, Nat. Commun. 10 (2019) 3145, https://doi.org/10.1038/s41467-019-10991-7.

[21] W.S. Yang, R. SriRamaratnam, M.E. Welsch, K. Shimada, R. Skouta, V. S. Viswanathan, J.H. Cheah, P.A. Clemons, A.F. Shamji, C.B. Clish, L.M. Brown, A. W. Girotti, V.W. Cornish, S.L. Schreiber, B.R. Stockwell, Regulation of ferroptotic cancer cell death by GPX4, Cell 156 (2014) 317–331, https://doi.org/10.1016/j.cell.2013.12.010.

[22] F. Ursini, M. Maiorino, Lipid peroxidation and ferroptosis: the role of GSH and GPx4, Free Radic. Biol. Med. 152 (2020) 175–185, https://doi.org/10.1016/j.freeradbiomed.2020.02.027.

[23] J.P. Friedmann Angeli, M. Schneider, B. Proneth, Y.Y. Tyurina, V.A. Tyurin, V. J. Hammond, N. Herbach, M. Aichler, A. Walch, E. Eggenhofer, D. Basavarajappa,

O. Radmark, S. Kobayashi, T. Seibt, H. Beck, F. Neff, I. Esposito, R. Wanke, H. Forster, O. Yefremova, M. Heinrichmeyer, G.W. Bornkamm, E.K. Geissler, S. B. Thomas, B.R. Stockwell, V.B. O'Donnell, V.E. Kagan, J.A. Schick, M. Conrad, Inactivation of the ferroptosis regulator Gpx4 triggers acute renal failure in mice, Nat. Cell Biol. 16 (2014) 1180–1191, https://doi.org/10.1038/ncb3064.

[24] D. Tang, X. Chen, R. Kang, G. Kroemer, Ferroptosis: molecular mechanisms and health implications, Cell Res. 31 (2021) 107–125, https://doi.org/10.1038/s41422-020-00441-1.

[25] M.J. Kerins, A. Ooi, The roles of NRF2 in modulating cellular iron homeostasis, Antioxidants Redox Signal. 29 (2018) 1756–1773, https://doi.org/10.1089/ars.2017.7176.

[26] Y. Li, T. Bao, W. Chen, Comparison of the protective effect of black and white mulberry against ethyl carbamate-induced cytotoxicity and oxidative damage, Food Chem. 243 (2018) 65–73, https://doi.org/10.1016/j.foodchem.2017.09.106.

[27] H. Su, Y. Li, D. Hu, L. Xie, H. Ke, X. Zheng, W. Chen, Procyanidin B2 ameliorates free fatty acids-induced hepatic steatosis through regulating TFEB-mediated lysosomal pathway and redox state, Free Radic. Biol. Med. 126 (2018) 269–286, https://doi.org/10.1016/j.freeradbiomed.2018.08.024.

[28] G.Q. Chen, F.A. Benthani, J. Wu, D. Liang, Z.X. Bian, X. Jiang, Artemisinin compounds sensitize cancer cells to ferroptosis by regulating iron homeostasis, Cell Death Differ. 27 (2020) 242–254, https://doi.org/10.1038/s41418-019-0352-3.

[29] S.J. Dixon, K.M. Lemberg, M.R. Lamprecht, R. Skouta, E.M. Zaitsev, C.E. Gleason, D.N. Patel, A.J. Bauer, A.M. Cantley, W.S. Yang, B. Morrison 3rd, B.R. Stockwell, Ferroptosis: an iron-dependent form of nonapoptotic cell death, Cell 149 (2012) 1060–1072, https://doi.org/10.1016/j.cell.2012.03.042.

[30] X. Jiang, B.R. Stockwell, M. Conrad, Ferroptosis: mechanisms, biology and role in disease, Nat. Rev. Mol. Cell Biol. 22 (2021) 266–282, https://doi.org/10.1038/s41580-020-00324-8.

[31] Y.P. Kang, A. Mockabee-Macias, C. Jiang, A. Falzone, N. Prieto-Farigua, E. Stone, I. S. Harris, G.M. DeNicola, Non-canonical glutamate-cysteine ligase activity protects against ferroptosis, Cell Metabol. 33 (2021) 174–189, https://doi.org/10.1016/j.cmet.2020.12.007, e177.

[32] Q. Ma, Role of nrf2 in oxidative stress and toxicity, Annu. Rev. Pharmacol. Toxicol. 53 (2013) 401–426, https://doi.org/10.1146/annurev-pharmtox-011112-140320.

[33] H.C. Huang, T. Nguyen, C.B. Pickett, Phosphorylation of Nrf2 at Ser-40 by protein kinase C regulates antioxidant response element-mediated transcription, J. Biol. Chem. 277 (2002) 42769–42774, https://doi.org/10.1074/jbc.M206911200.

[34] D.A. Bloom, A.K. Jaiswal, Phosphorylation of Nrf2 at Ser40 by protein kinase C in response to antioxidants leads to the release of Nrf2 from INrf2, but is not required for Nrf2 stabilization/accumulation in the nucleus and transcriptional activation of antioxidant response element-mediated NAD(P)H:quinone oxidoreductase-1 gene expression, J. Biol. Chem. 278 (2003) 44675–44682, https://doi.org/10.1074/jbc.M307633200.

[35] T. Wang, F. Dai, G.H. Li, X.M. Chen, Y.R. Li, S.Q. Wang, D.M. Ren, X.N. Wang, H. X. Lou, B. Zhou, T. Shen, Trans-4, 4′-dihydroxystilbene ameliorates cigarette smoke-induced progression of chronic obstructive pulmonary disease via inhibiting oxidative stress and inflammatory response, Free Radic. Biol. Med. 152 (2020) 525–539. https://10.1016/j.freeradbiomed.2019.11.026.

[36] M. Theodore, Y. Kawai, J. Yang, Y. Kleshchenko, S.P. Reddy, F. Villalta, I.J. Arinze, Multiple nuclear localization signals function in the nuclear import of the transcription factor Nrf2, J. Biol. Chem. 283 (2008) 8984–8994, https://doi.org/10.1074/jbc.M709040200.

[37] G.T. Stathopoulos, T.P. Sherrill, D.S. Cheng, R.M. Scoggins, W. Han, V. V. Polosukhin, L. Connelly, F.E. Yull, B. Fingleton, T.S. Blackwell, Epithelial NF-kappaB activation promotes urethane-induced lung carcinogenesis, Proc. Natl. Acad. Sci. U. S. A. 104 (2007) 18514–18519, https://doi.org/10.1073/pnas.0705316104.

[38] C. Narayan, A. Kumar, Constitutive over expression of IL-1beta, IL-6, NF-kappaB, and Stat3 is a potential cause of lung tumorgenesis in urethane (ethyl carbamate) induced Balb/c mice, J. Carcinog. 11 (2012) 9, https://doi.org/10.4103/1477-3163.98965.

[39] B.R. Sharma, T.D. Kanneganti, NLRP3 inflammasome in cancer and metabolic diseases, Nat. Immunol. 22 (2021) 550–559, https://doi.org/10.1038/s41590-021-00886-5.

[40] G. Szabo, T. Csak, Inflammasomes in liver diseases, J. Hepatol. 57 (2012) 642–654, https://doi.org/10.1016/j.jhep.2012.03.035.

[41] M. Balamurugan, P. Santharaman, T. Madasamy, S. Rajesh, N.K. Sethy, K. Bhargava, S. Kotamraju, C. Karunakaran, Recent trends in electrochemical biosensors of superoxide dismutases, Biosens. Bioelectron. 116 (2018) 89–99, https://doi.org/10.1016/j.bios.2018.05.040.

[42] M. Pajares, A. Cuadrado, N. Engedal, Z. Jirsova, M. Cahova, The role of free radicals in autophagy regulation: implications for ageing, Oxid. Med. Cell. Longev. (2018) 2450748, https://doi.org/10.1155/2018/2450748, 2018.

[43] S.C. Andrews, The Ferritin-like superfamily: evolution of the biological iron storeman from a rubrerythrin-like ancestor, Biochim. Biophys. Acta 1800 (2010) 691–705, https://doi.org/10.1016/j.bbagen.2010.05.010.

[44] A. Ayala, M.F. Munoz, S. Arguelles, Lipid peroxidation: production, metabolism, and signaling mechanisms of malondialdehyde and 4-hydroxy-2-nonenal, Oxid. Med. Cell. Longev. (2014) 360438, https://doi.org/10.1155/2014/360438, 2014.

[45] X. Fang, H. Wang, D. Han, E. Xie, X. Yang, J. Wei, S. Gu, F. Gao, N. Zhu, X. Yin, Q. Cheng, P. Zhang, W. Dai, J. Chen, F. Yang, H.T. Yang, A. Linkermann, W. Gu, J. Min, F. Wang, Ferroptosis as a target for protection against cardiomyopathy, Proc. Natl. Acad. Sci. U. S. A. 116 (2019) 2672–2680, https://doi.org/10.1073/pnas.1821022116.

[46] A. Jelinek, L. Heyder, M. Daude, M. Plessner, S. Krippner, R. Grosse, W. E. Diederich, C. Culmsee, Mitochondrial rescue prevents glutathione peroxidase-dependent ferroptosis, Free Radic. Biol. Med. 117 (2018) 45–57, https://doi.org/10.1016/j.freeradbiomed.2018.01.019.

[47] K.V. Swanson, M. Deng, J.P. Ting, The NLRP3 inflammasome: molecular activation and regulation to therapeutics, Nat. Rev. Immunol. 19 (2019) 477–489, https://doi.org/10.1038/s41577-019-0165-0.

[48] P. Gurung, J.R. Lukens, T.D. Kanneganti, Mitochondria: diversity in the regulation of the NLRP3 inflammasome, Trends Mol. Med. 21 (2015) 193–201, https://doi.org/10.1016/j.molmed.2014.11.008.

[49] J. Kim, M. Xu, R. Xo, A. Mates, G.L. Wilson, A.W.t. Pearsall, V. Grishko, Mitochondrial DNA damage is involved in apoptosis caused by pro-inflammatory cytokines in human OA chondrocytes, Osteoarthritis Cartilage 18 (2010) 424–432, https://doi.org/10.1016/j.joca.2009.09.008.

[50] A. Guidarelli, L. Cerioni, O. Cantoni, Inhibition of complex III promotes loss of Ca2 + dependence for mitochondrial superoxide formation and permeability transition evoked by peroxynitrite, J. Cell Sci. 120 (2007) 1908–1914, https://doi.org/10.1242/jcs.003228.

[51] S.S. Xie, Y. Deng, S. Guo, et al., Endothelial cell ferroptosis mediates monocrotaline-induced pulmonary hypertension in rats by modulating NLRP3 inflammasome activation, Sci. Rep. 12 (1) (2022) 1–16, https://doi.org/10.1038/s41598-022-06848-7.

[52] T. Zhang, H. Tsutsuki, W. Islam, et al., ATP exposure stimulates glutathione efflux as a necessary switch for NLRP3 inflammasome activation, Redox Biol. 41 (2021) 101930, https://doi.org/10.1016/j.redox.2021.101930.

[53] M.M. Hughes, A. Hooftman, S. Angiari, et al., Glutathione transferase omega-1 regulates NLRP3 inflammasome activation through NEK7 deglutathionylation, Cell Rep. 29 (1) (2019) 151–161, https://doi.org/10.1016/j.celrep.2019.08.072, e5.

[54] Y. Huang, W. Xu, R. Zhou, NLRP3 inflammasome activation and cell death[J], Cell. Mol. Immunol. 18 (9) (2021) 2114–2127, https://doi.org/10.1038/s41423-021-00740-6.

[55] F. Wang, Y. Liu, J. Yuan, W. Yang, Z. Mo, Compound C protects mice from HFD-induced obesity and nonalcoholic fatty liver disease, Internet J. Endocrinol. (2019) 3206587, https://doi.org/10.1155/2019/3206587, 2019.

[56] F. Ursini, M. Maiorino, M. Valente, L. Ferri, C. Gregolin, Purification from pig liver of a protein which protects liposomes and biomembranes from peroxidative degradation and exhibits glutathione peroxidase activity on phosphatidylcholine hydroperoxides, BBA-Lipid Lipid Met. 710 (1982) 197–211, https://doi.org/10.1016/0005-2760(82)90150-3.

[57] F. Ursini, M. Maiorino, C. Gregolin, The selenoenzyme phospholipid hydroperoxide glutathione peroxidase, BBA-Gen Subjects 839 (1985) 62–70, https://doi.org/10.1016/0304-4165(85)90182-5.

[58] F.G. Guengerich, D.H. Kim, Enzymic oxidation of ethyl carbamate to vinyl carbamate and its role as an intermediate in the formation of 1 N6-ethenoadenosine, Chem. Res. Toxicol. 4 (1991) 413–421, https://doi.org/10.1021/tx00022a003.

[59] F.P. Guengerich, D.H. Kim, M. Iwasaki, Role of human cytochrome P-450 IIE1 in the oxidation of many low molecular weight cancer suspects, Chem. Res. Toxicol. 4 (1991) 168–179, https://doi.org/10.1021/tx00020a008.

[60] R.A. Kemper, S.R. Myers, H.E. Hurst, Detoxification of vinyl carbamate epoxide by glutathione: evidence for participation of glutathione S-transferases in metabolism of ethyl carbamate, Toxicol. Appl. Pharmacol. 135 (1) (1995) 110–118, https://doi.org/10.1006/taap.1995.1213.

[61] S.C. Lu, Regulation of glutathione synthesis, Mol. Aspect. Med. 30 (2009) 42–59.

[62] S.J. Dixon, D.N. Patel, M. Welsch, R. Skouta, E.D. Lee, M. Hayano, A.G. Thomas, C. E. Gleason, N.P. Tatonetti, B.S. Slusher, B.R. Stockwell, Pharmacological inhibition of cystine-glutamate exchange induces endoplasmic reticulum stress and ferroptosis, Elife 3 (2014), e02523, https://doi.org/10.7554/eLife.02523.

[63] X. Sun, Z. Ou, R. Chen, X. Niu, D. Chen, R. Kang, D. Tang, Activation of the p62-Keap1-NRF2 pathway protects against ferroptosis in hepatocellular carcinoma cells, Hepatology 63 (2016) 173–184, https://doi.org/10.1002/hep.28251.

[64] Y. Xie, S. Zhu, X. Song, X. Sun, Y. Fan, J. Liu, M. Zhong, H. Yuan, L. Zhang, T. R. Billiar, M.T. Lotze, H.J. Zeh 3rd, R. Kang, G. Kroemer, D. Tang, The tumor suppressor p53 limits ferroptosis by blocking DPP4 activity, Cell Rep. 20 (2017) 1692–1704, https://doi.org/10.1016/j.celrep.2017.07.055.

[65] J. Lu, Y. Zhao, M. Liu, J. Lu, S. Guan, Toward improved human health: Nrf2 plays a critical role in regulating ferroptosis, Food Funct. 12 (2021) 9583–9606, https://doi.org/10.1039/d1fo01036k.

[66] A.M. Koorts, M. Viljoen, Ferritin and ferritin isoforms I: structure-function relationships, synthesis, degradation and secretion, Arch. Physiol. Biochem. 113 (2007) 30–54, https://doi.org/10.1080/13813450701318583.

[67] M.K. Kwak, K. Itoh, M. Yamamoto, T.R. Sutter, T.W. Kensler, Role of transcription factor Nrf2 in the induction of hepatic phase 2 and antioxidative enzymes in vivo by the cancer chemoprotective agent, 3 H-1, 2-dithiole-3-thione, Mol. Med. 7 (2001) 135–145, https://doi.org/10.1177/1532673X12437555.

[68] R.K. Thimmulappa, K.H. Mai, S. Srisuma, T.W. Kensler, M. Yamamoto, S. Biswal, Identification of Nrf2-regulated genes induced by the chemopreventive agent sulforaphane by oligonucleotide microarray, Cancer Res. 62 (2002) 5196–5203, https://doi.org/10.1002/cncr.10878.

[69] E.C. Pietsch, J.Y. Chan, F.M. Torti, S.V. Torti, Nrf2 mediates the induction of ferritin H in response to xenobiotics and cancer chemopreventive dithiolethiones, J. Biol. Chem. 278 (2003) 2361–2369, https://doi.org/10.1074/jbc.M210664200.

[70] Q. Wang, C. Bin, Q. Xue, Q. Gao, A. Huang, K. Wang, N. Tang, GSTZ1 sensitizes hepatocellular carcinoma cells to sorafenib-induced ferroptosis via inhibition of NRF2/GPX4 axis, Cell Death Dis. 12 (2021) 1–16, https://doi.org/10.1038/s41419-021-03718-4.